*Pharmaceutical Research, Vol. 22, No. 11, November 2005 (© 2005)*
DOI: 10.1007/s11095-005-7750-6

*Research Paper*

# Pharmacokinetic–Pharmacodynamic Modeling of the Hydroxy Lerisetron Metabolite L6-OH in Rats: An Integrated Parent–Metabolite Model

**Fátima Ortega,[1,2] Antonio Quintana,[1] Elena Suárez,[1] John C. Lukas,[1,3] Nerea Jauregizar,[4] Leire de la Fuente,[4] Maria Luisa Lucero,[5] Ana Gonzalo,[5] Aurelio Orjales,[5] and Rosario Calvo[1,6]**

*Received February 10, 2005; accepted August 2, 2005*

***Purpose.*** The twofold aim of this study was to characterize *in vivo* in rats the pharmacokinetics (PK) and pharmacodynamics (PD) of L6-OH, a metabolite of lerisetron with *in vitro* pharmacological activity, and evaluate the extent to which L6-OH contributes to the overall effect.
***Methods.*** The PK of L6-OH was determined directly postmetabolite i.v. dose (PK-1), and also simultaneously for L (lerisetron concentration) and for generated L6-OH after lerisetron dose (200 μg $kg^{-1}$, i.v.), using Nonlinear Mixed Effects Modeling with an integrated parent–metabolite PK model (PK-2). Surrogate effect was measured by inhibition of serotonin-induced bradycardia. Protein binding was assayed via ultrafiltration and all quantification was performed via liquid chromatography-electrospray ionization-mass spectrometry.
***Results.*** L6-OH showed elevated plasma and renal clearances, and volume of distribution (PK-1). The *in vivo* potency (PD) of L6-OH was high ($EC_{50}$ = 0.098 ng $mL^{-1}$ and $EC_{50unbound}$ = 0.040 ng $mL^{-1}$). Total clearance for L (PK-2) in the presence of generated L6-OH ($CL_L = CL_{\rightarrow L6\text{-}OH} + CL_n$) was 0.0139 L $min^{-1}$. Most of this clearance was L6-OH formation ($F_c$ = 99.6%), but only an 8.6% fraction of L6-OH was released into the bloodstream. The remainder undergoes biliar and fecal elimination. The parameters estimated from PK-2 were used to predict concentrations of L6-OH ($Cp_{L6}$) generated after a lerisetron therapeutic dose (10 μg $kg^{-1}$) in the rat. These concentrations are needed for the PD model and are below the quantification limit. $Cp_{L6max}$ was less than the $EC_{50}$ of L6-OH.
***Conclusions.*** We conclude that after lerisetron administration, L6-OH is extensively formed in the rat but it is quickly eliminated; therefore, besides being equipotent with the parent drug, the L6-OH metabolite does not influence the effect of lerisetron.

**KEY WORDS:** integrated parent metabolite model; lerisetron; metabolite; pharmacokinetic.

## INTRODUCTION

In the initial phases of drug development, it is important to know the metabolic pattern of the new agent, particularly for compounds susceptible to metabolizing into pharmacologically active elements. The 5-$HT_3$ antagonists are such compounds. These drugs were developed as antiemetics, for the treatment of vomiting secondary to chemotherapy or radiation in cancer therapy (1,2). In general, the 5-$HT_3$ antagonists have elevated clearance and short half-life, but their duration of effect is generally longer than half-life-related estimates and it varies between compounds (3). The majority of these antagonists have metabolites with affinity for the 5-HT3 receptor, and the possible contribution of these metabolites to the total duration of the antiemetic effect has been contemplated. Interest on this facet of the elimination process has increased after the introduction of new 5-$HT_3$ antagonits, such as granisetron (4), tropisetron (5), and dolasetron (6). However, little is known about the potency and the intrinsic activity *in vivo* of the metabolites, or to what extent they contribute to the global pharmacological effect of the parent agent. To estimate the influence of an active metabolite on the global activity of a drug, the combined pharmacokinetics/pharmacodynamics (PK/PD) of the metabolite must be characterized after its direct administration in pure form (7,8). Nevertheless, in the development stages, this is complicated due to nonavailability of synthesized metabolites.

Lerisetron (L) is a new highly selective and potent serotonin 5-$HT_3$ receptor antagonist, currently in phase III of development for clinical use as an antiemetic (9). This drug possesses high affinity binding for the 5-$HT_3$ receptors ($pK_i$ = 9.2) as well as a potent ability ($ED_{50}$ = 2 μg $kg^{-1}$, i.v.) to

[1] Department of Pharmacology, University of the Basque Country, Leioa, Vizcaya, Spain.
[2] Dynakin SL, Parque Tecnologico de Vizcaya, Edificio 801-A, Derio, Vizcaya, Spain.
[3] Pharsight Corp., Mountain View, CA, USA.
[4] PharmaDatum Data Analysis, S.L.L., Edificio BEAZ, Sondika, Vizcaya, Spain.
[5] Department of Research, FAES FARMA, S.A., Maximo Aguirre 14, Leioa, Vizcaya, Spain.
[6] To whom correspondence should be addressed. (e-mail: rcalvo@lg.ehu.es)

inhibit the von Bezold–Jarisch (B–J) reflex in anesthetized rats (10). This surrogate reflex is extensively used to investigate the mode of action of 5-$HT_3$ receptor antagonism in rodents (11,12). It has been observed that the hydroxy derivative in position 6 of lerisetron (L6-OH) has pharmacological activity *in vitro* ($pK_i$ = 9; $ED_{50}$ = 1 μg $kg^{-1}$, i.v.) (10). In addition, this metabolite has been detected in plasma and urine in healthy volunteers after oral administration of lerisetron (internal documentation of FAES FARMA S.A., Leioa, Vizcaya, Spain).

The PK of lerisetron, after i.v. administration in the rat, has already been studied (13–15). At least one metabolite seemed to be formed after lerisetron ($^{14}C$ lerisetron) i.v., because (1) the area under the curve (AUC) of total plasma radioactivity lerisetron (TL) was higher than the AUC of the parent compound (L); (2) the duration of the effect was above that expected based on the half-life alone ($t_{1/2}\beta$ = 30 min); and (3) in spite of the above, the potency of TL to inhibit the B–J reflex was less than that calculated from the parent drug alone ($EC_{50}$ = 0.88 *vs.* 0.44 ng $mL^{-1}$). These earlier studies seem to indicate either the presence of nonactive metabolites [according to item (3)] or the possible coexistence of active and inactive metabolites (i.e., conjugated metabolites) [according to items (1) and (2)].

The hydroxy metabolite is currently available in pure form. In this work, our aim was to (1) determine the PK of the hydroxy metabolite (and also examine its pharmacological activity) after direct administration of L6-OH in the rat; (2) develop an integrated PK model, for the parent drug as well as the metabolite, allowing evaluation in PD of the metabolite contribution to the overall effect of lerisetron.

## MATERIALS AND METHODS

### Drugs and Reagents

Lerisetron and its metabolites, L6-OH and L5-OH, were synthesized by FAES FARMA S.A. laboratories. $^{14}C$ Lerisetron hydrochloride (specific activity, 28.07 mCi $mM^{-1}$) was obtained from Huntingdon Life Sciences (Alconbury, UK). Radiochemical purity was over 98%. Desipramine hydrochloride, used as internal standard in the analytic procedure, was obtained from Sigma-Aldrich Química S.A. (Barcelona, Spain). For the enzymatic hydrolysis of the metabolites, β-D-glucuronidase from *Escherichia coli*, type IX-A (activity, 3000 U $mL^{-1}$), was purchased from Sigma-Aldrich. Chemicals for HPLC analyses were at least of HPLC grade. All other reagents and solvents were procured from commercial sources.

### Animals

For the experiments, male Sprague–Dawley rats ($n$ = 66; 215–298 g) were used. The rats were assigned into seven groups (A, B, C, D, E, F, and G) and doses were administered intravenously (i.v.) as follows: qualitative metabolite characterization of lerisetron post 200 μg $kg^{-1}$, i.v. (group A: $n$ = 4); PK of lerisetron post 200 μg $kg^{-1}$ (group B: $n$ = 16); urine and feces with $^{14}C$ lerisetron at 200 μg $kg^{-1}$ (group C: $n$ = 4); PK of L6-OH at 10 μg $kg^{-1}$ (group D: $n$ = 7) and at 200 μg $kg^{-1}$ (group E: $n$ = 5); protein plasma binding for L6-OH (group F: $n$ = 8) and pharmacological effect of L6-OH (group G: $n$ = 22). This last group observed was after 0.3, 1, 3, 5, and 10 μg $kg^{-1}$ doses of L6-OH, similar to the ones used for the B–J reflex with L (14). The subgroup of the 3 μg $kg^{-1}$ dose ($n$ = 5) was arbitrarily set aside for PK-1/PD model validation (validation subgroup).

The rats were maintained under laboratory standard conditions on a 12 h light/dark cycle, with light from 8:00 A.M. to 8:00 P.M., in a temperature (21–22°C)- and humidity (70%)-controlled room, and were acclimated a minimum of 4 days before experiments were performed. Food (standard laboratory rat, mouse, and hamster diets; Panlab, Barcelona, Spain) and water were available *ad libitum*. The protocol of the study was approved by the Committee on Animal Experimentation of the University of the Basque Country. The day before the experiment, animals were fasted overnight. All experiments were started between 9:00 and 10:00 A.M. to exclude influences of circadian rhythms.

### Study Design for Metabolism and PK Studies

#### *Intravenous Administration of Lerisetron*

Initially, plasma (1–60 min) and urine (to 48 h) samples from group A, after i.v. administration of lerisetron, were used for qualitative metabolite characterization of L. Next, rats (group B: 240–264 g) were used for quantification of plasma levels of L and its L6-OH metabolite, after lerisetron (200 μg $kg^{-1}$; mean dose = 52.72 μg).

On the day before the assay, rats were anesthetized with ether. Jugular catheters (polyethylene catheters $PE_{10}$, 0.28 mm i.d., 10 cm length; Vygon, Ecouen, France) for drug administration and intraarterial carotid catheters ($PE_{50}$, 0.58 mm i.d., 10 cm length) for blood sample withdrawal, respectively, were implanted. Before dosing, plasma and urine were collected. In group B, between two and five arterial blood samples were collected at intervals from 1 to 180 min postdose and placed in heparinized tubes. A volume of blood of 0.4 mL was drawn from each animal and at each sampling time to provide sufficient drug for detection. Blood was replaced with an equal volume of saline. The maximum total amount of blood withdrawn was 2 mL per rat. Plasma was separated by centrifugation at 2500 rpm, 37°C for 15 min. After the first 15 min of blood collection, rats ($n$ = 11 out of the 16 in this group) (mean dose 52.60 μg) were placed in metabolic cages (and blood collection continued) for urine collection during a period of 48 h. All samples were stored at −20°C until assay of lerisetron and metabolites by liquid chromatography (LC)-electrospray ionization (ESI)-mass spectrometry (MS). Two rats of group B were placed in metabolism cages and were used for collection of feces for a period of 48 h.

#### *$^{14}C$ Lerisetron i.v. Administration for the Determination of Total Radioactivity in Urine and Feces*

On the day before the assay, the rats of group C (205–212 g) were anesthetized with ether and jugular catheters ($PE_{10}$) for drug administration were implanted. On the day of the study, the rats received 200 μg $kg^{-1}$ of $^{14}C$ lerisetron (mean dose = 42.15 μg) and were placed in metabolic cages for urine and feces collection over a period of 144 h. The

urine and feces samples were stored at 2°C until radioactivity analysis.

*Direct Intravenous Administration of L6-OH Metabolite*

The PK of L6-OH was determined in group D and group E (215–267 g). Group D received 10 μg $kg^{-1}$ (mean dose = 2.43 μg) and group E 200 μg $kg^{-1}$, i.v. (mean dose = 46.19 μg) of L6-OH, so that linearity of the PK of the metabolite could be established by comparing the parameters after these two doses. The dose amounts were selected, by approximation, based on the results from group B. The experimental protocol was the same as for groups A and B. Arterial blood samples were collected at intervals from 1 to 120 min postdose and placed in heparinized tubes. Plasma was separated by centrifugation and all samples were stored at −20°C until analysis for L6-OH metabolite by LC ESI-MS. Three of the rats from group E, receiving 44.69 μg average, were placed in metabolic cages for urine sample collection during 56 h to be used in the calculation of $CL_{renal}$ ($CL_r$) for L6-OH.

**Analytical Techniques**

*Plasma, Urine, and Feces Sample Treatment Prior to LC-ESI-MS*

For qualitative identification of lerisetron metabolites, plasma samples (0.2 mL) from group A were separated in two aliquots of 0.1 mL. One of them was extracted by a liquid–liquid extraction procedure with sodium hydroxide 0.1 M and *tert*-butyl methyl ether, and then reconstituted in 90 μL of ammonium acetate/acetic acid buffer (20 mM, pH = 4) and 10 μL desipramine as internal standard (from a 1 μg $mL^{-1}$ solution in ammonium acetate/acetic acid buffer), so the final internal standard concentration in the sample was 100 ng $mL^{-1}$. A 75-μL aliquot was taken and 50 μL was injected into the LC-ESI-MS system. For the identification of glucuronide metabolites, other aliquots of 0.1 mL of plasma were incubated with β-D-glucuronidase (activity 3000 $UmL^{-1}$) at 37°C, 90 min (previously optimized), and then extracted with the same liquid–liquid extraction procedure.

For qualitative identification of metabolites, aliquots of 0.2 mL of urine from group A were diluted with the same volume of ammonium acetate/acetic buffer (pH = 4) and directly injected into the LC-ESI-MS system set in Full Scan acquisition detection mode. Other 0.2-mL aliquots of urine were incubated with β-D-glucuronidase (activity 3000 U $mL^{-1}$) at 37°C, 60 min (previously optimized), for the identification of glucuronide metabolites and then extracted with the liquid–liquid extraction procedure.

The quantitation of lerisetron and L6-OH levels in plasma and urine from groups B, D, and E was performed in aliquots of 0.2 mL extracted by the liquid–liquid extraction procedure and reconstituted in 190 μL of ammonium acetate/acetic acid buffer (20 mM, pH = 4) and 10 μL of internal standard desipramine (from a 2 μg $mL^{-1}$ solution in ammonium acetate/acetic acid buffer), so the final internal standard concentration in the sample was 100 ng $mL^{-1}$. A 150-μL aliquot was taken and 100 μL was injected into the LC-ESI-MS system. For the quantitation of glucuronide from L6-OH (L6-Ogluc), aliquots of 0.2 mL of urine from groups B and E were incubated with β-D-glucuronidase based on the criteria described above. The fecal samples were homogenized with methanol and internal standard. Subsequently, they were centrifuged and an aliquot of the supernatant was filtered before direct injection in the quantification system.

*LC-ESI-MS Conditions*

An ion trap mass spectrometer (Finnigan LCQ, Thermo Electron Corp., Waltham, MA, USA) was interfaced with an HPLC system consisting of Spectra System P2000 pump and a Spectra System AS3000 autosampler (Thermo Electron Corp.) fitted with a 200-μL sample loop. The compounds were separated on a Symmetry Shield RP8 column (5 μm particle size, 250 × 4.6 mm; Waters Corp., Milford, MA, USA). The mobile phase consisted of ammonium acetate/acetic acid buffer (20 mM, pH = 4) (solvent A) and acetonitrile (solvent B). The flow gradient was initially 90:10 (v/v) of A:B, linearly ramped to 70:30 over 10 min and then to 0:100 over 5 min, and returned to 90:10 over 5 min. This condition was further held for 2 min prior to the injection of another sample. The total chromatographic run time was 22 min. The flow rate was 1 mL $min^{-1}$ at a column temperature of 30°C (Modality 1). To prevent equipment degradation, a split of the column eluant was included so that only 0.5 mL $min^{-1}$ entered the mass spectrometer that operated at atmospheric pressure ionization and was fitted with an ESI source (Modality 2). This modality was used when the quantification level was high.

The MS was operated in the positive ion ESI mode. Initially, a Full Scan detection mode was used in the range of 100–600 $m/z$ (mass-to-charge ratio) in the qualitative analysis of plasma (extracted samples) and urine (extracted and diluted with buffer samples) from group A.

The detection of compounds in samples from groups A, B, D, and E were performed by selected reaction monitoring (SRM) mode. The ion transitions monitored were 309.3–218.1 $m/z$ for L6-OH metabolite, 293.3–201.2 $m/z$ for lerisetron, and 267.3–236.1 $m/z$ for the internal standard desipramine. Additionally, in urine samples diluted with buffer (direct injection), the ion transition monitored for the glucuronide metabolites was 485.2–309.2 $m/z$. Hellium was used as the collision gas in the ion trap and the optimum relative collision energies for the selected transitions were found to be 24% for L, 22.5% for L6-OH, 20% for glucuronide metabolites, and 16% for desipramine. Data acquisition was in the positive ionization centroid mode using the LCQ software system for data processing.

*Calibration Curves and Assay Validation After LC-ESI-MS Analysis*

Stock solutions of L and L6-OH were made in 90% pure water–10% acetonitrile by dissolving accurately weighed amounts of compounds. The stock solution of desipramine (internal standard) was made in pure water. The spiked plasma and urine standard curve and plasma and urine quality control samples were made from stock solution by serial dilution with pure water.

The percent of relative extraction (liquid–liquid) recovery of L and L6-OH metabolite from plasma was >95% and

from urine it was >72%. The variability of L and L6-OH in the extraction process of the standard curves introduced each day of the experiment did not exceed 10% in the range of 0.01–200 ng $mL^{-1}$ for L and 0.02–200 ng $mL^{-1}$ for L6-OH in plasma ($n = 5$, for three concentrations in each range). For the urine samples, the range was 0.3–500 ng $mL^{-1}$ for L and 0.65–4000 ng $mL^{-1}$ for L6-OH.

Calibration curves were constructed by plotting the peak-area ratios from chromatograms of lerisetron or L6-OH over internal standard *versus* the concentrations of lerisetron or L6-OH, respectively. In plasma-extracted samples, the lower limit of quantification was 0.01 ng $mL^{-1}$ for lerisetron and 0.02 ng $mL^{-1}$ for L6-OH metabolite in modality 1, and 0.2 and 0.5 ng $mL^{-1}$ for L and L6-OH in modality 2. In urine-extracted samples, the limit of quantification was 0.3 ng $mL^{-1}$ for lerisetron and 0.65 ng $mL^{-1}$ for L6-OH (modality 2). In feces, the limit was 1 and 2 ng $mL^{-1}$ for L and L6-OH, respectively.

The analytical methodology was validated according to the procedure agreed upon during the consensus meeting on "Analytical methods validation: bioavailability, bioequivalence and pharmacokinetic studies" and "Bioanalytical methods validation—a revisit with a decade of progress" (16). The intraday and interday accuracy and precision of the analytical method were both <15%.

### *$^{14}C$ Lerisetron Assay*

Aliquots of rat urine (100 μL) were placed in vials to which scintillation counting liquid (10 mL of Cocktail Biogreen 1) was added and the radioactivity was counted by a Packard Tricarb model 2200 CA (Packard Instrument Co. Inc., Meriden, CT, USA). Aliquots of feces were placed in vials, 3 mL of tissue solvent Ti 350 was added, and the vials were maintained at 37°C during 24 h. At an environmental temperature, 10 mL of scintillation liquid was added and the whole mixture placed in vials and maintained at 2–4°C for 24 h. Radioactivity was determined by a Packard Tricarb model 2200 CA (Packard Instruments). The detection limit of $^{14}C$ lerisetron was 0.5 ng $mL^{-1}$.

### *In Vitro Protein Binding Study*

*In vitro* plasma L6-OH binding was investigated in a separate set of rats (group F; $n = 8$) via an ultrafiltration method using an Amicon MPS-1 (Millipore Corporation, Billerica, MA, USA) micropartition device. L6-OH [final concentration ($C$) of 10, 50, and 100 mg $mL^{-1}$] was added (10 μL) to plasma (990 μL) collected from rats ($n = 5$). The adsorption of L6-OH to the ultrafiltration device and membrane over the concentration range of L6-OH from 10 to 100 ng $mL^{-1}$ was negligible. The ultrafiltration conditions were as previously described for lerisetron (17). The free concentration obtained as ultrafiltrate (Cu) was measured by direct injection in the LC-ESI-MS system described above. With each series of samples, vials containing aliquots of the ultrafiltrate and known quantities of the L6-OH metabolite in the range 1–80 ng $mL^{-1}$ were used as standards. The limit of detection of the assay was 1 ng $mL^{-1}$. The unbound fraction in plasma (fu) was determined as, fu = Cu/$C$.

The effect of L on protein binding of L6-OH was also studied in a parallel experiment ($n = 3$), where plasma samples (980 μL) were preincubated with 10 μL of L (final concentration, 100 ng $mL^{-1}$) for 10 min. These were then spiked with up to 10 μL of L6-OH (final concentration of 10, 50, and 100 ng $mL^{-1}$) and binding determination was as described above.

## Assay for the Pharmacological Activity of L6-OH

Rats (231–298 g) of group G were allocated randomly into five subgroups and fasted overnight before the experiment. At the time of the experiment rats were anesthetized with urethane (1.25 g $kg^{-1}$, i.p.; Sigma-Aldrich). After a surgical incision in the throat, a polyethylene tube was introduced and fixed into the trachea to aid ventilation in the spontaneously breathing animal. A polyethylene catheter ($PE_{50}$), filled with heparinized saline (50 IU heparin $mL^{-1}$ physiological saline solution; Rovi, Barcelona, Spain), was placed into the right carotid artery and connected to a pressure transducer (Abbott Critical Care, Sligo, Ireland) that was coupled to a MacLab/4e system. Arterial blood pressure and heart rate were monitored using a computer (Macintosh Performa 5200) and the complete experiment was recorded on disk for further analysis and evaluation. Another polyethylene catheter ($PE_{10}$) was placed and fixed into the right jugular vein to perform drug administration. A heated pad was used to maintain the animal temperature at 37°C throughout the experiment.

In preliminary experiments, we studied the dose–response relationship for serotonin-induced bradycardia (as part of the B–J reflex) in the range 4–128 μg $kg^{-1}$ i.v. administered at 10- to 15-min intervals. A dose of 16 μg $kg^{-1}$, i.v. ($n = 4$), of 5-HT resulted in a submaximal reproducible response over a 4-h period when administered at the above intervals so this dose of 5-HT was used throughout the present study for induction of the B–J reflex. After completion of the catheter placement, animals were allowed to stabilize during a 30-min period. This period was followed by a challenge with 5-HT that was repeated three times at 10-min intervals to establish the control bradycardic response as the index (basal heart rate − 5-HT rate) / (basal heart rate). Then, the metabolite L6-OH was administered as i.v. bolus (doses of 0.3, 1, 3, 5, and 10 μg $kg^{-1}$), and the degree of inhibition of the bradycardic response to 5-HT was checked at 5, 15, 30, 45, 60, 90, 120, 150, 180, 210, and 240 min afterwards in each dose.

## Data Analysis

### *PK Analysis*

Initially, noncompartmental analysis was used to analyze the observations in groups D and E to test for linearity using naïve pooling (WinNonlin® 1.5, Pharsight Inc., Mountain View, CA, USA). The estimated PK parameters were systemic plasma clearance (CL), area under the plasma concentration–time curve from time 0 to infinity ($AUC_{0-\infty}$), and volume of distribution at steady state ($V_{ss}$).

L plasma concentration (Cp) *versus* time (group B) (ignoring the presence of L6-OH) were analyzed using a

mixed effects procedure for compartmental modeling [Nonlinear Mixed Effects Modeling (NONMEM) Project group, University of San Francisco, San Francisco, CA, USA]. The method obtains the population distribution of the PK parameters and that of the intraindividual variability error, separately (14,15). The L6-OH concentration ($Cp_{L6}$) *versus* time (group E) (PK-1) were also analyzed with NONMEM. Because of the large number of data points ($n$ = 28) *versus* individual rats ($n$ = 5), a standard two-stage (STS)-like approach was used (providing no precision estimates). In this method, each individual rats PK model parameters are estimated and the normal assumption is used to approximate the dispersion (standard deviation or coefficient of variation).

Compartmental modeling diagnostics was based on various criteria: (1) a significant change in the NONMEM objective function, (2) distribution of the weighted residuals *versus* the prediction, and (3) improvement in the precision of the estimates. A bicompartmental model (Model PK-1) optimally fitted the individual concentration *versus* time data from each group. The intercompartmental mass transfer rates $k_{12}$, $k_{21}$, elimination rate $k_{10}$, CL, and central volume of distribution ($V_c$) were estimated as primary parameters. Steady-state volume ($V_{ss}$) and mean residence time (MRT = $V_{ss}$/CL), were calculated.

Unbound PK parameters of L6-OH and lerisetron were calculated by dividing the total parameters by the fu value previously obtained *in vitro* from group F for L6-OH, and as obtained earlier for L (fu = 14%) (14).

### *PD Analysis of L6-OH*

A dose–response curve was created from effect measurements after L6-OH metabolite administration. The response observed at 15 min after i.v. doses of 0.3, 1, 3, 5, and 10 μg $kg^{-1}$ of metabolite were used to estimate the $ED_{50}$ (the dose at half-maximal effect). PK parameter estimates of L6-OH from group E (200 μg $kg^{-1}$), after direct metabolite i.v., were used to simulate the concentrations at the times and doses of the effects (0.3, 1, 5, and 10 μg $kg^{-1}$) because, at these doses, nonquantifiable concentrations were obtained. Effect measurements were performed in anesthetized rats, as it had been previously verified (13–15) that there are no significant parameter differences between anesthetized and awake rats.

The effect–concentration relationship (PD) was analyzed with WinNonlin and was visibly nonlinear. An $E_{max}$ sigmoid model and a simple $E_{max}$ model were tested for best fit and selection was made on the basis of the Akaike Information Criterion (AIC). Model diagnosis was also performed by visual analysis of the weighted residual plots, and by observation of the CV% of the estimated parameters.

The effect was related to simulated plasma metabolite L6-OH concentrations by the sigmoid $E_{max}$ relation,

$$E = E_{max}\frac{Cps^{\gamma}}{EC_{50}^{\gamma} + Cps^{\gamma}} \quad (1)$$

where $E$ is the modeled effect, Cps is the simulated concentration at the time of the response observation, $E_{max}$ is the maximum effect, $EC_{50}$ is the metabolite concentration in plasma at half maximal effect, and γ (the Hill exponent) is related to the number of binding sites per receptor molecule for the particular drug and determines the sigmoidicity of the curve. The PD parameters (γ and $EC_{50}$) obtained with this model after fitting the pooled doses of 0.3, 1, 5, and 10 μg $kg^{-1}$ were used to simulate effect *versus* time at the 3 μg $kg^{-1}$ dose for validation of the PK/PD model.

After administration of L (and subsequent generation of L6-OH), synergistic effect models were not applied because preliminary observations showed that the generated L6-OH concentrations were below the putative *in vitro* potency.

### *Validation of PK and PD of L6-OH*

The concentration and effect time courses were simulated for a 3 μg $kg^{-1}$ L6-OH metabolite dose based on the parameters from PK-1 and PD, and then compared (18) with the observed effect evolution in the randomly selected validation subgroup.

### *Lerisetron and L6-OH Metabolite Integrated PK Model (Model PK-2)*

The concentration *versus* time profiles of lerisetron and its L6-OH metabolite, formed after lerisetron administration (group B: 200 μg $kg^{-1}$), were best described by using an integrated bicompartmental model with metabolite formation. The final modeling scheme is shown in Fig. 1. Initially, a simple (nonbiliary submodel) metabolite elimination model (parallel bicompartmental representation) was attempted, with the bile, feces, and urine compartments turned off.

Based on the observations, the elevated metabolic clearance of L was not reflected in measurement of A. The final model system used to describe the central (Ac) and peripheral (Ap) compartments for L, the central (Am) and peripheral ($Am_2$) compartments for L6-OH, as well as the gall bladder (Ag), feces (for L6-OH) (Af), and urine + feces (for L) (Auf) compartments was

$$\frac{dAc}{dt} = -k_{12}Ac + k_{21}Ap - \left(\frac{CL_L}{V_c}\right)Ac \quad (2)$$

$$\frac{dAp}{dt} = -k_{21}Ap + k_{12}Ac \quad (3)$$

$$\frac{dAm}{dt} = \left(\frac{[1-F_m]CL_{\rightarrow L6\text{-}OH}}{V_c}\right)Ac - k_{m2}Am + k_{2m}Am_2 - \left(\frac{CL_{mt}}{V_m}\right)Am \quad (4)$$

$$\frac{dAm_2}{dt} = -k_{2m}Am_2 + k_{m2}Am \quad (5)$$

$$\frac{dAg}{dt} = \left(\frac{F_m CL_{\rightarrow L6\text{-}OH}}{V_c}\right)Ac - k_{56}Ag \quad (6)$$

$$\frac{dAf}{dt} = k_{56}Ag \quad (7)$$

$$\frac{dAuf}{dt} = \left(\frac{CL_n}{V_c}\right)Ac \quad (8)$$

$$CL_L = CL_{\rightarrow L6\text{-}OH} + CL_n \quad (9)$$

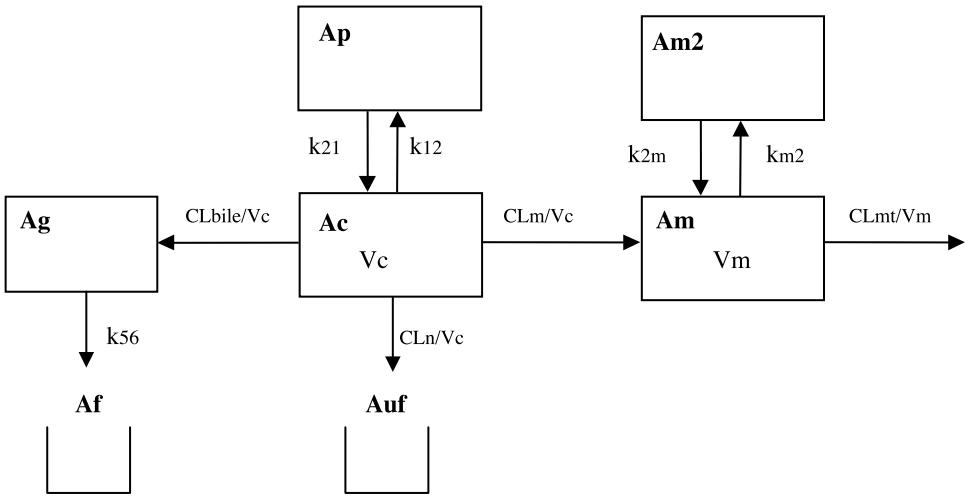


**Fig. 1.** Schematic representation of a dual bicompartmental model for L and its metabolite L6-OH after intravenous (200 μg $kg^{-1}$) administration of lerisetron, as represented in NONMEM. The input to the L6-OH side is the fraction of lerisetron converted into metabolite ($F_m$). Ac, Am and Ap, Am2 are amounts in the central and peripheral L and L6-OH compartments, respectively. Ag is a gallbladder compartment, and Af and Auf are compartments for feces collection of L6-OH and nonmetabolic (urine + feces) for L. $CL_{bile} = F_m \times CL_{\rightarrow L6\text{-}OH}$ is clearance of L metabolized to L6-OH towards a gallbladder compartment, $CL_m = (1 - F_m) \times CL_{\rightarrow L6\text{-}OH}$ is the clearance of L metabolized to L6-OH into other systemic L6-OH elimination and $CL_n$ nonmetabolic L clearance; $CL_{mt}$ is L6-OH clearance. $V_c$ and $V_m$ are L and L6-OH central volumes of distribution, respectively.

$CL_L$ is the total systemic clearance of L, $CL_{\rightarrow L6\text{-}OH}$ is the clearance of L by transformation into L6-OH alone, $CL_{bile} = F_m * CL_{\rightarrow L6\text{-}OH}$, and $CL_m = (1 - F_m) * CL_{\rightarrow L6\text{-}OH}$ are the clearances of L transformed in L6-OH from the central compartment to the bile ("first pass"-like elimination), and that following the elimination course of L6-OH but through the bloodstream, respectively. $CL_n$ is the clearance of L not into L6-OH (renal clearance and/or other metabolic pathways). $CL_{mt}$ is the elimination clearance of the L6-OH metabolite. $V_c$ and $V_m$ are central volumes of distribution for L and L6-OH, respectively. The intercompartmental transfer rates $k_{12}$ and $k_{21}$ are for the parent, and $k_{2m}$ and $k_{m2}$ for the metabolite, central to peripheral compartments, and for one-way gall bladder to excretion in feces ($k_{56}$). Af and Auf were introduced in the model as observed amounts and are discussed below. The initial, nonbiliary first-pass elimination submodel, included only Eqs. (2), (3), (4), and (5) with $F_m = 0$, which then collapses $CL_{bile} = 0$ and $CL_m = CL_{\rightarrow L6\text{-}OH}$.

$F_m$ in the model is an estimated parameter, but it can be approximated from the observations as

$$1 - F_m = \frac{\text{AUC}_{\text{generated L6-OH}}}{\text{AUC}_{\text{injected L6-OH}}} \tag{10}$$

Initial estimates for model parameters were obtained for L from group B. The bicompartmental PK model parameters for L6-OH were obtained from the direct administration study (group E, 200 μg $kg^{-1}$) and were initially fixed in the integrated model (7,19). The parameters $CL_n$ and $k_{56}$ were also fixed after direct calculation from data obtained in urine and feces, respectively. In subsequent fits, the deep compartment transfer rates for L6-OH were left to vary and estimated during model fitting.

The clearance of L corresponding to L6-OH formation alone $CL_{\rightarrow L6\text{-}OH}$, as estimated in the integrated model, was used to calculate the corresponding conversion fraction into L6-OH

$$F_c = \frac{CL_{\rightarrow L6\text{-}OH}}{CL_{\rightarrow L6\text{-}OH} + CL_n} \tag{11}$$

Subsequently, the parameters estimated from PK-2 were used to predict generated $Cp_{L6}$ after a therapeutic lerisetron dose (10 μg $kg^{-1}$). This permits estimation of the influence of the active metabolite on the global effect of the parent drug.

## RESULTS

### Metabolism Study

In plasma, after i.v. lerisetron administration (group A, qualitative study), two hydroxy metabolites were detected. Only one of them showed quantifiable levels corresponding to the compound hydroxylated at position 6 of the original drug, L6-OH. In the chromatogram of Fig. 2A, a visible separation of the products is seen for L6-OH (e.g., at 9.44 min), L5-OH, L, and internal standard at 14.96 min. These two metabolites, having the same mass, were identified depending on their retention times by comparison with the reference chromatograms. Incubation of plasma samples with β-glucuronidase also showed the qualitative existence of conjugated metabolite resulting from phase II metabolism (conjugated L6-OH, L6-Ogluc).

Both L6-OH and its corresponding conjugate were detected in urine samples collected from 0 to 48 h after lerisetron administration. In the chromatogram of Fig. 2B, a visible separation is seen for the four products (L6-Ogluc,

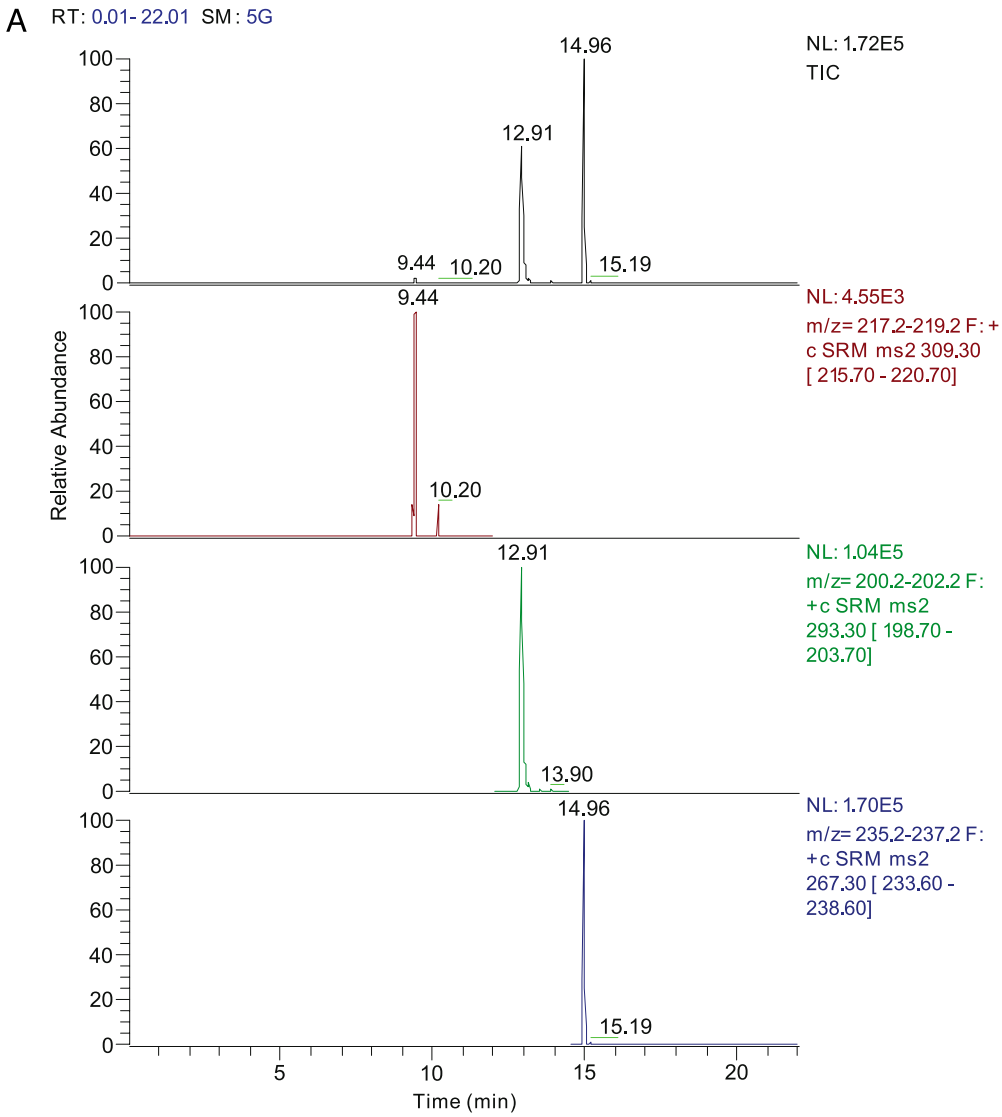


**Fig. 2.** (A) SRM chromatograms corresponding to a plasma sample in the rat obtained at 5 min post 200 μg $kg^{-1}$ lerisetron (i.v.). The upper frame shows all cromatography peaks obtained during 22 min. The remaining chromatograms show the specific peaks corresponding to the fragments of each compound: L6-OH metabolite (9.44 min), L5-OH (10.20 min), lerisetron (12.91 min), and internal standard (14.96 min). (B) SRM chromatogram corresponding to a urine sample in the rat, collected in the 0- to 24-h interval post i.v. administration of lerisetron, diluted with buffer. The peaks of L6-Ogluc (4.33 min), L5-Ogluc (7.15 min), L6-OH (11.04 min), L5-OH (11.89 min), lerisetron (14.48 min), and internal standard (15.32 min) are seen.

L5-Ogluc, L6-OH, L5-OH, L, internal standard). A full-scan analysis did not reveal the presence of any other compounds. Figure 3 shows the metabolic scheme for lerisetron in rat.

### Pharmacokinetics of Lerisetron in Plasma and Urine

The observations of Cp *versus* time for L after lerisetron administration (group B, 200 μg $kg^{-1}$) are shown in Fig. 4, together with the model mean prediction (PK-1). The insert depicts L6-OH ($Cp_{L6}$) levels, across a 100-fold reduced *y*-scale, generated after lerisetron administration. The assay levels beyond 120 min were near or below the quantification limit with large variability, so the analysis covers from 0 to 120 min postdose. The $AUC_{0-\infty}$ below the generated $Cp_{L6}$ curve was 43.4 μg min $L^{-1}$ *versus* 5400 μg min $L^{-1}$ for L and 2067 μg min $L^{-1}$ for L6-OH after injection of metabolite. The PK of lerisetron, ignoring L6-OH (PK-1), coincided with the literature (14) and were (typical value [$CI_{95\%}$]), $CL_L$ = 0.0162 (0.0008, 0.031) L $min^{-1}$, $V_c$ = 0.276 (0.270, 0.281) L. The unbound parameters for L were $CL_u$ = 0.12 L $min^{-1}$ and $V_u$ = 1.97 l.

The amounts recovered in urine (Table I) indicate that renal clearance ($CL_r$) is low ($2.6 \times 10^{-5}$ L $min^{-1}$) (0.14 μg recovered in 48 h of a total of 52.60 μg administered). Comparing this with the systemic plasma $CL_L$ of lerisetron, it is deduced that a significant amount of lerisetron is eliminated via nonrenal routes. The amount recovered in feces (mean of two rats) for L was 0.12 and 12 μg for L6-OH

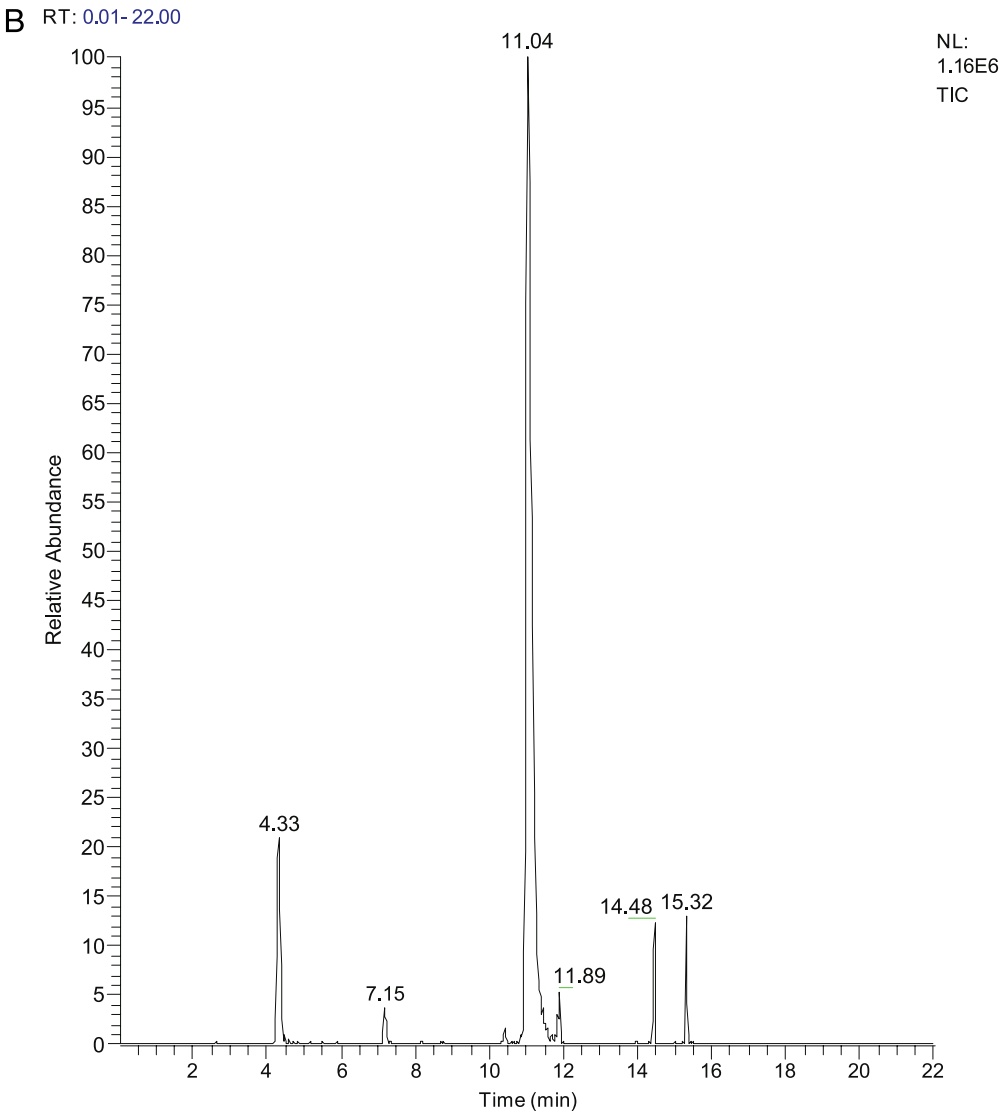


**Fig. 2.** Continued.

($CL_{feces}$ = 2.2 × $10^{-5}$ L $min^{-1}$). The remainder of clearance (~0.016 L $min^{-1}$) must be attributable to metabolism. In the integrated model, the total observed amount for non-metabolic depletion of L (feces + urine = 0.26 μg) appears in compartment Auf. Excretion in feces of L6-OH is included in Af.

Table I also lists the results obtained from urine and feces after $^{14}C$ lerisetron (mean dose = 42.15 μg). As was expected, a significant amount of lerisetron is eliminated in feces. The amount recovered in urine of $^{14}C$ lerisetron was 8.12 μg (compared to 0.14 μg of L); therefore most of renal clearance corresponds to the possible metabolites.

### Metabolic and PK Study of L6-OH

Noncompartmental PK analysis of L6-OH was used to verify linearity in the 10–200 μg $kg^{-1}$ dose (i.v.) range, and so the remaining study was performed with the 200 μg $kg^{-1}$ dose (group E). Linearity was confirmed because the dose-corrected AUC, the CL, and Vss were not different within that dose range (e.g., CL was 0.022 *versus* 0.023 L $min^{-1}$, at 10 and 200 μg $kg^{-1}$, respectively).

The observed plasma concentrations ($Cp_{L6}$) and mean bicompartmental model fits *versus* time of L6-OH, after direct administration (200 μg $kg^{-1}$ of L6-OH), are shown in Fig. 5 (group E). The PK parameter estimates are listed in Table II. L6-OH distributes to a large central volume and it is also rapidly eliminated. The metabolite also showed elevated $CL_r$ (5.8 × $10^{-3}$ L $min^{-1}$), although the total collected in urine (26.67% of the total 44.69 μg) indicates important nonrenal elimination similarly to lerisetron. These parameters (given proof of linearity) can be used to simulate the PK at doses that produce effect, but whose concentration levels are below the quantification limit and are needed to perform the PK/PD analysis relating concentration to effect.

Linearity in protein binding was also assessed in the entire dose range. The average L6-OH unbound percent in rat plasma is 41 ±1.6%. In presence of L, fu was 63±2.5%. The unbound drug parameters, listed in Table II, were obtained by dividing the corresponding parameter for total (bound and

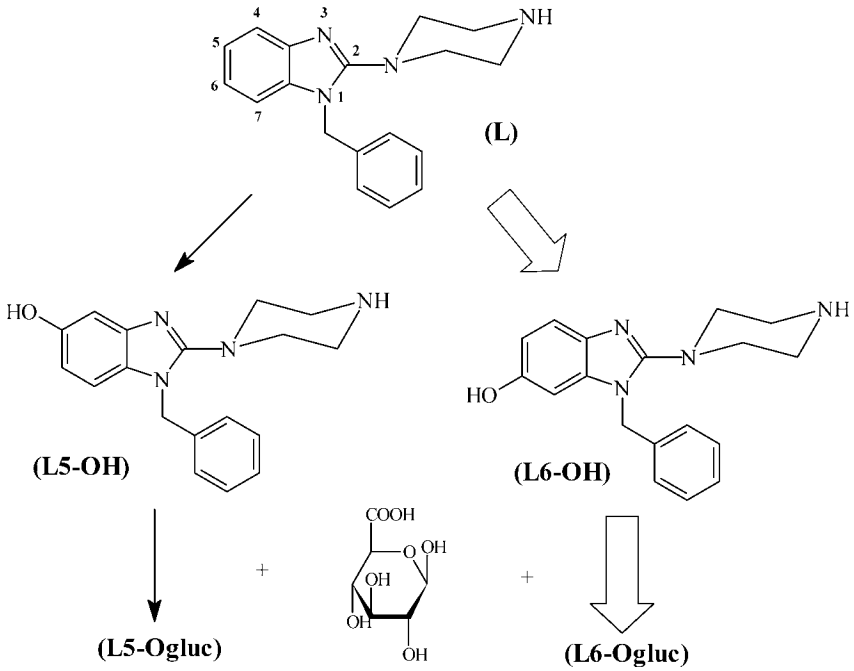


**Fig. 3.** Proposed metabolic scheme of lerisetron in Sprague–Dawley rats with the principal pathway (wide arrows) into L6-OH.

unbound) L6-OH by the fu. Both $V_u$ (unbound volume of distribution) and $CL_u$ (unbound CL) were elevated. All PK parameters between L and L6-OH differed, and notably the $V_u$ for L6-OH is much lower than that for L (1.97 l for L *versus* 0.36 l for L6-OH).

### *In Vivo* Drug Effect

Figure 6 shows measurements (mean ± SEM) of the time course of bradycardia inhibition after administration of five distinct doses of L6-OH. It is clear that (1) the effect is dose-dependent at least with the B–J reflex surrogate, (2) and L6-OH causes rapid suppression of bradycardia. Also, in the insert, effect estimated at 15 min postdose is depicted *versus* dose for L (solid line) and L6-OH (dotted line). Here, it is obvious (3) that L6-OH has a high potency ($ED_{50} \approx 0.43$ μg kg$^{-1}$).

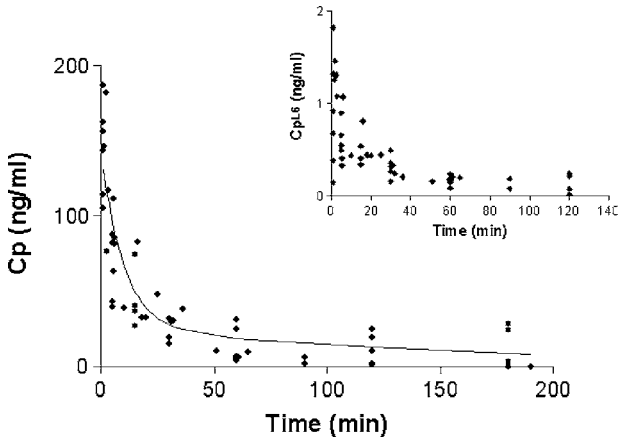


**Fig. 4.** Plasma concentration *vs.* time profiles of L (Cp) (solid symbols) after intravenous administration of lerisetron (200 μg kg$^{-1}$) in group B of rats ($n$ = 16). The bicompartmental model-predicted concentration profile (solid line) of lerisetron is also shown. Insert: observed plasma concentrations ($Cp_{L6}$) of L6-OH secondary to lerisetron.

### Concentration Effect Relationship (PD)

Figure 7A depicts bradycardia inhibition observations *versus* total simulated plasma concentrations (Cps) and PD model (Eq. 1) best fits after lerisetron and L6-OH doses. Figure 7B shows the expected effect after fitting the model of Eq. (1) to the unbound concentrations. For lerisetron, PD parameters and observations were obtained from an earlier study (14) and are listed in Table III, together with the PD parameter estimates for L6-OH. We have not performed synergistic PD modeling (or derived the PD parameters for L) because of the low concentrations reached in the central compartments by L6-OH. We remark that there is a significant difference ($p < 0.0001$) in potencies ($EC_{50}$) between L and L6-OH, but when expressed as the unbound parameter ($EC_{50u}$), the two were equal (Table III) (Fig. 7).

The PK and PD parameters of L6-OH were used to *a priori* predict the effect after L6-OH dosing in the validation subgroup. There were no significant differences between

**Table I.** Amounts (μg) of L, L6-OH, and L6-Ogluc (Mean ± SD), Post 52.60 μg Mean Lerisetron Dose, Recovered in Urine (Group B; $n$ = 11) and Feces (Group B; $n$ = 2 out of 11) after 48 h. Also, Recovery in Urine and Feces Post 42.15 μg $^{14}$C Lerisetron Administration after 144 h (Group C; $n$ = 4)

| Sample | Lerisetron | L6-OH | L6-Ogluc | Total |
|---|---|---|---|---|
| Urine | 0.14 ± 0.16 | 2.32 ± 1.66 | 6.54 ± 4.41 | 9.01 ± 5.96 |
| Feces | 0.12 | 12 | – | 12.12 |
| $^{14}$C urine | 8.12 ± 1.55 | – | – | 8.12 ± 1.55 |
| $^{14}$C feces | 26.01 ± 8.95 | – | – | 26.01 ± 8.95 |

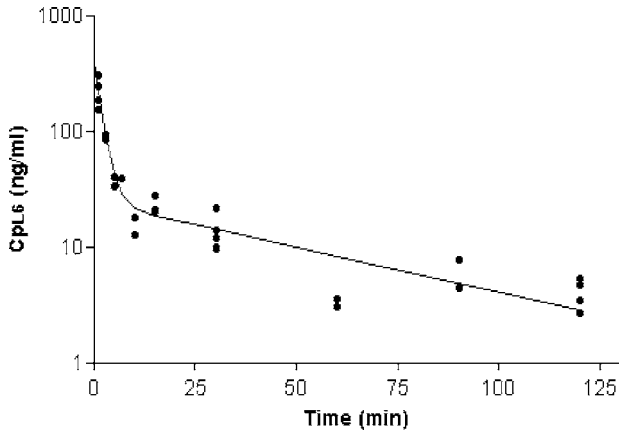


**Fig. 5.** Plasma concentration ($Cp_{L6}$) *vs.* time profiles of L6-OH, after direct i.v. administration of the pure L6-OH metabolite (200 μg $kg^{-1}$) in group E ($n$ = 5). Observations (solid circles) and the bicompartmental model-predicted $Cp_{L6}$ profile (solid line) of L6-OH are shown ($log_{10}$ $y$-axis).

observations and the prediction ($p > 0.05$). Mean prediction error bias was [mean (95% confidence interval)], −1.64 (−7.13 to 3.84), and precision was 20.18%.

### Integrated Parent–Metabolite Model (PK-2)

The concentration–time profiles of L were simultaneously analyzed with those of L6-OH formed post-lerisetron dose (group B). Initially, all PK parameters of L6-OH (metabolite compartments) were fixed to those obtained from separate administration, and $F_m$, an analog of bioavailability, was estimated in the fit. This approach led to unstable fits with failing covariance step. As metabolite elimination is formation rate limited (8), only CL and V were eventually fixed and the intercompartmental rates left to vary.

**Table II.** Standard Two-Stage (from NONMEM) Bicompartmental Model PK Parameters and Interanimal Coefficient Percent for the L6-OH Metabolite After Direct i.v. Dose of 200 μg $kg^{-1}$ of L6-OH Metabolite (Group E; $n$ = 5)

| | Estimate (CV%) |
|---|---|
| PK parameter | |
| $CL_{mt}$ (L $min^{-1}$) | 0.027 (28%) |
| $V_m$ (L) | 0.146 (37%) |
| $k_{m2}$ ($min^{-1}$) | 0.401 (16%) |
| $k_{2m}$ ($min^{-1}$) | 0.072 (17%) |
| Calculated parameters | |
| $k_{10}$ ($min^{-1}$) | 0.185 |
| $CL_r$ (L $min^{-1}$) | 0.0058 |
| $CL_{nr}$ (L $min^{-1}$) | 0.0212 |
| $AUC_{0-\infty}$ (μg min $L^{-1}$) | 2067 ± 257 |
| fu[a] | 0.410 ± 0.016 |
| $CL_u$ (L $min^{-1}$) | 0.066 |
| $V_u$ (L) | 0.36 |

Algebraically derived parameters of interest are also listed: renal clearance, $CL_r$ = mean amount recovered in urine/AUC; $CL_{nr}$ = $CL_{mt}$ − $CL_r$. The area under the concentration–time curve (AUC) and the unbound fraction (fu), estimated *in vitro*, are listed with their standard deviations.

[a] fu obtained in the presence of lerisetron was 0.63 ± 0.025.

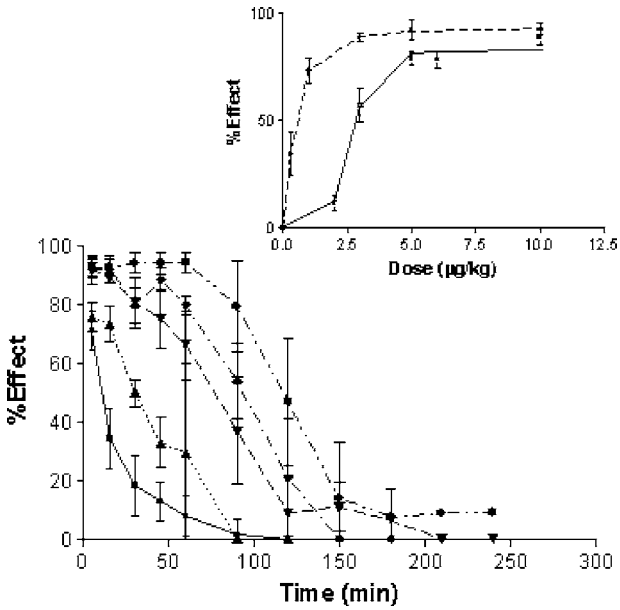


**Fig. 6.** Time course of L6-OH effect (mean ± SEM). The response measured is serotonin-induced bradycardia (von Bezold–Jarisch reflex) inhibition after i.v. bolus of L6-OH metabolite to Sprague–Dawley rats of 0.3 μg $kg^{-1}$ (squares) ($n$ = 4), 1 μg $kg^{-1}$ (upright triangles) ($n$ = 5), 3 μg $kg^{-1}$ (inverted triangles) ($n$ = 5), 5 μg $kg^{-1}$ (rhomboids) ($n$ = 4), 10 μg $kg^{-1}$ (circles) ($n$ = 4). The insert shows the effect as a function of lerisetron dose (open squares) (2, 3, 5, 6, and 10 μg $kg^{-1}$) (PD data from Jauregizar *et al.* [14]) and L6-OH doses (solid circles) (0.3, 1, 3, 5, and 10 μg $kg^{-1}$).

The simple parent–metabolite (two compartments each) model provided unrealistic parameter estimates for the metabolite clearance ($CL_{mt}$ ~ 0.41 L $min^{-1}$ ≫ physiological hepatic flux in the rat of 0.013 L $min^{-1}$). When this parameter was fixed, there was a clear bias in the residuals. It became obvious that a more complex model was required to explain the low observed levels metabolite in spite of its elevated formation deduced from the high metabolic clearance of parent (discussed above). An appropriate model seems one incorporating a biliary "first pass," so that the metabolite, immediately after generation in the liver, is eliminated via the biliary route into the feces. In spite of the lack of observations in the bile compartment, for physiological similarity, this compartment appears in the system. The rate of transfer out of the bile was estimated using time course measurements in a feces compartment.

The NONMEM parameter estimates are listed in Table IV. Total CL for L ($CL_L$ = $CL_{\rightarrow L6\text{-}OH}$ + $CL_n$) as well the volume of distribution and the other parameters were similar to those obtained ignoring the generation of L6-OH (PK-1) (Table II). The table also lists the model parameter estimate for $F_m$ (Eq. 10) and the calculated value for the fraction $F_c$ (Eq. 11). Figure 8 shows the integrated model fit to the observations of L6-OH generated post-L (200 μg $kg^{-1}$, i.v.) administration and for an average dose of 52.72 μg.

Two approaches were used in integrated modeling: (1) fixing the parameters of L6-OH to those obtained after direct administration; (2) fixing the parameters of L6-OH but corrected to account for the difference in protein binding in the presence of the parent drug, L (63% *versus* 41% without the parent). As objective function was smaller for approach

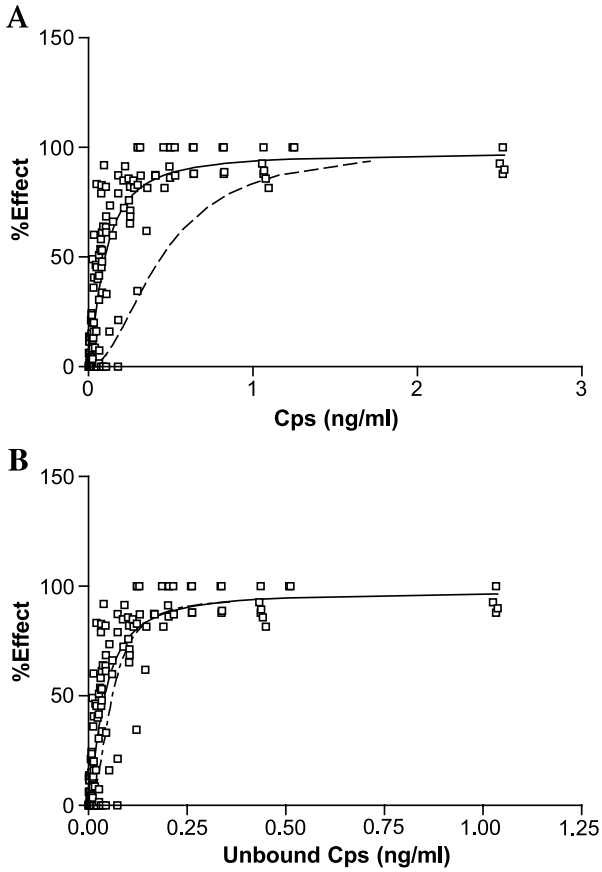


**Fig. 7.** (A) PD plot of von Bezold–Jarisch effect for lerisetron and L6-OH as a function of simulated concentrations in plasma (Cps). For lerisetron, the model prediction from PD parameters is shown (dotted line). For L6-OH, observations at doses 0.3, 1, 5, and 10 μg $kg^{-1}$ (open squares) and model fits (Table III) (solid line) are depicted. (B) Same as (A) but relating unbound Cps with effect.

(1), and this was verified by the typical model diagnostics, Table IV therefore lists the total estimates.

Finally, the PK and PD parameter estimates were used to simulate the concentrations of generated metabolite and its corresponding effect–time profiles, following a lerisetron dose in the lerisetron range used for the effect measurement (10 μg $kg^{-1}$) (Fig. 9). As can be deduced from the $Cp_{L6}$ magnitudes in the figure, the contribution of L6-OH in the global effect of lerisetron must be low, because the $C_{max}$ observed lies below the $EC_{50}$ of L6-OH (0.098 ng $mL^{-1}$).

## DISCUSSION

Approximately 40% (20) of attrition in the drug development process is attributable to pharmacokinetics, either because of incomplete studies or because the new molecules eventually fail in that respect. In particular, metabolites may be active and also interfere with the kinetics or dynamics of the drug. In earlier studies in the rat, it was observed that lerisetron had elevated plasma clearance (14) that was apparently related to extensive hydroxylation. The other $5HT_3$ antagonists commonly used in the clinic, e.g., ondansetron, granisetron, tropisetron, and dolasetron, are also metabolized by hydroxylation as the major metabolic route (4–6,21,22). Ample metabolism is typically associated to short half-lives, but if the effect lasts longer, the existence of active metabolites may well be suspected to play a role.

The fact that many of these metabolites are active has major implications on the overall PK/PD of the drug, and its modeling, with particular difficulty in the early phases of drug development, because of the lack of pure metabolite. In the case of lerisetron, various compounds were available and therefore the PK and PD of the major metabolite, L6-OH, could be characterized after i.v. administration.

### PK and Elimination Behavior of Lerisetron

The PK parameters obtained in this work for L were of the same order as in a previous study using a different analytical method (13–15). The initial concentrations of generated metabolite L6-OH in plasma, secondary to i.v. administration of lerisetron, were about 100 times lower than those corresponding to L, with the $AUC_{0-\infty}$ of L6-OH at 0.8% of that corresponding to L. The low levels of L6-OH observed in plasma ($Cp_{L6}$) is in contrast with the amount of L6-OH in feces (which was much higher than the level expected from $Cp_{L6}$). Reasons for the low plasma levels may relate to (1) the fact that the L6-OH metabolite is not formed in considerable quantities, which seems to contradict with the supposedly extensive metabolism of lerisetron as well as with the high levels of L6-OH and conjugate detected in urine after L dosing, and that (2) L6-OH, once formed, is rapidly eliminated through the biliar route from the organism of the rat.

With respect to assumption (1), experiments with $^{14}C$ lerisetron were performed because elimination in feces could not be rejected. The mean quantity of radioactivity recovered in urine (8.12 μg) in a period of 144 h after $^{14}C$ lerisetron administration (sum of unaltered lerisetron, and all possible metabolites) corresponds to 19.21% of the administered dose similar to the 16.72% total amount recovered in urine after L (sum of unaltered lerisetron, L6-OH, and L6-Ogluc). It can be concluded that lerisetron is principally transformed to the L6-OH metabolite, and from this to L6-Ogluc, and that there is no unidentified metabolite that could significantly contribute to the total amounts excreted, except for small quantities of the L5-OH metabolite and its glucuronide L5-Ogluc. However, the mean amount of radioactive substance recovered in feces (26.01 μg) in the same period (144 h) post-$^{14}C$ lerisetron dose corresponded to 62.04% of the mean

**Table III.** Naïve Pooled Pharmacodynamic Parameters (Precision of the Estimate %) of the Metabolite ($n$ = 17) and Lerisetron (see [14]) ($n$ = 31)

| PD parameter | L6-OH metabolite | Lerisetron |
|---|---|---|
| $E_{max}$ (%) | 97.45 (5%) | 100[a] |
| $EC_{50}$ (ng $mL^{-1}$) | 0.098 (12%)** | 10.44 (5.9%) |
| γ | 1.39 (13%) | 2.0 (12%) |
| $EC_{50}u$ (ng $mL^{-1}$)[b] | 0.040 (12.5%) | 0.064 (15.6%) |

[a] Fixed to 100.
[b] Calculated as unbound parameter = (total parameter) × (fu).
**$p < 0.0001$.

**Table IV.** Typical PK Parameters for L in the Presence of L6-OH from Integrated (Fig. 1) Parent–Metabolite Modeling in NONMEM (PK-2)

L—model side[a]

| Symbol | $CL_L$ (L $min^{-1}$) | $V_c$ (L) | $k_{12}$ ($min^{-1}$) | $k_{21}$ ($min^{-1}$) | $F_m$ | $CL_n$ (L $min^{-1}$) | $k_{56}$ ($min^{-1}$) |
|---|---|---|---|---|---|---|---|
| Parameter estimate | 0.0139 | 0.281 | 0.165 | 0.117 | 0.914 | [0.00005][b] | [0.000081] |
| Precision of the estimate | 13% | 7.2% | 27% | 19% | 30% | – | – |
| Interindividual variability (IIV%) | 47% | 12% | – | – | – | – | – |
| Precision of the IIV estimate (%) | 26% | 7.5% | – | – | – | – | – |

L6-OH—model side

| Symbol | $CL_{mt}$ (L $min^{-1}$) | $V_m$ (L) | $k_{m2}$ ($min^{-1}$) | $k_{2m}$ ($min^{-1}$) | $\varepsilon$[c] |
|---|---|---|---|---|---|
| Parameter estimate | [ 0.027 ] | [ 0.146 ] | 0.006 | 1.18 | 55% |
| Precision of the estimate | – | – | 39% | 25% | 51% |
| Interindividual variability (IIV%) | [28%][d] | [37%] | – | – | – |

$F_c$ = 99.6% and 1 − $F_m$ = 8.6%.
[a] Mixed residual error model for the parent: constant coefficient of variation − proportional residual error = 13.7%; additive error = 3.43 ng $mL^{-1}$.
[b] [ ]: parameter fixed in the final fits.
[c] Constant coefficient of variation—proportional residual error for the metabolite side.
[d] Fixed to the approximate estimates from standard two-stage fits (no precision estimates) of the L6-OH kinetics after direct injection (group E).

administered dose, and this suggests that lerisetron is eliminated preferably by feces, or the biliary rather than the renal route.

Although it may seem unusual that a drug administered i.v. could be eliminated principally in feces, this process has been described for other drugs, such as lesopitron (23), and may associate to various eventualities: (1) The L parent is excreted directly in feces through an active efflux transport mechanism, e.g., P-glycoprotein (P-gp) (24). Indeed, some antagonists of $5HT_3$ are known substrates of this protein (e.g., ramosetron) (25). (2) One of the hydroxy metabolites (L6-OH) may be a substrate for P-gp and is eliminated as it is formed, without excluding an interaction with L at the P-gp transport level. (3) What appears in feces is one of the conjugated metabolites eliminated through the bile, or it is L6-OH. With the measurement in feces of 12 μg L6-OH, which does not correspond to the AUC (in plasma) of generated metabolite of 43 μg min $L^{-1}$, it was confirmed that L6-OH is eliminated from the bile directly and almost entirely to feces, which shows a connection to suggestion (2).

## PK and PD Characterization Post i.v. Administration of the L6-OH Metabolite

L6-OH showed bicompartmental behavior with elevated CL and V resulting in short $t_{1/2}\alpha$ and $t_{1/2}\beta$ of L6-OH, much lower than for lerisetron (1.2 and 41.6 *versus* 6.7 and 110 min, respectively). The MRT was 41.6 min for L6-OH and 127.5 min for lerisetron. The metabolite is removed more rapidly from the organism compared to L, so elimination of L6-OH is formation rate-limited.

Protein binding of L6-OH was 41%, and $V_u$ and $CL_u$ reveal extensive distribution and metabolism. The former is a better approximation of the volume where the drug would be distributed, were it not bound to protein, and the latter approximates the intrinsic clearance and is similar to that *in vitro* at microsome level. Compared to L, $V_u$ of L6-OH is almost five times smaller and results in much higher initial unbound concentrations (pharmacologically active form); nevertheless, it is subsequently eliminated rapidly—as seen in the evolution of total amounts in urine and feces.

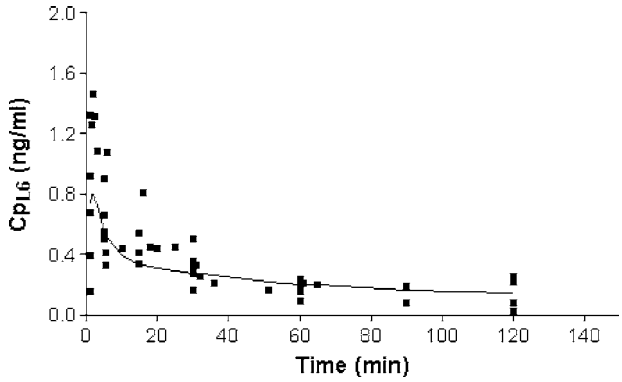


**Fig. 8.** Plasma concentration ($Cp_{L6}$) time course of generated L6-OH after a dose of 200 μg $kg^{-1}$ lerisetron (i.v.) (52.72 μg average dose, group B). Symbols are experimental observations and the line represents the integrated parent–metabolite model fit for generated L6-OH.

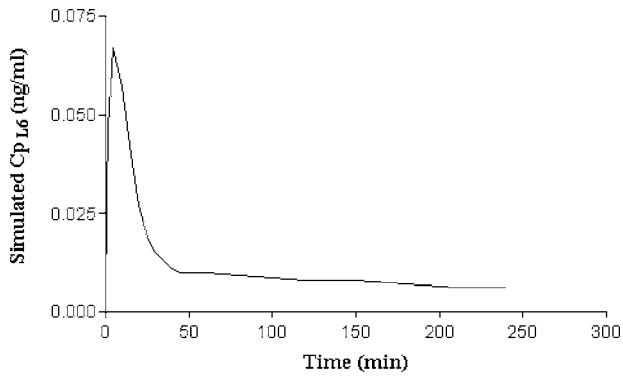


**Fig. 9.** Simulation of the temporal evolution of L6-OH plasma concentrations ($Cp_{L6}$) based on integrated parent–metabolite model parameters (Table IV) after a dose in the therapeutic range of 10 μg $kg^{-1}$ lerisetron (i.v.) (mean dose = 2.7 μg) in rats.

After direct i.v. dose of L6-OH, its $CL_r$ became elevated, higher than that of lerisetron (0.026 mL $min^{-1}$) and closer to the renal blood flow in the rat (9 mL $min^{-1}$). This suggests that renal excretion of the metabolite could be associated to an active transport process.

### Metabolite Effect

To measure the metabolite effect, a previously validated surrogate effect was used. Preclinical PK/PD modeling using surrogate endpoints or biomarkers is widely regarded as potentially beneficial in all phases of drug development. This approach enables the prediction of pharmacological response in humans.

In this work, as expected from the *in vitro* studies, the L6-OH compound had pharmacological effect *in vivo*, as registered in dose–response curves. It shows rapid initiation of action, but also rapid recovery. $ED_{50}$ of the two compounds, obtained 15 min postdose i.v., was six times smaller for L6-OH than for lerisetron (2.65 μg $kg^{-1}$) (14). When estimated at 5 min postdose, the potency seemed to increase by 16-fold for L6-OH. However, this is not certain, because $ED_{50}$ depends on PK, which can differ between compounds, especially for unbound concentrations. The $V_u$ of L6-OH was lower than for L, with higher initial concentrations; however, these are subsequently compensated for by the rapid distribution and elimination rates as reflected in the MRT for L6-OH. Therefore, in comparative PD studies *in vivo*, it is important to take into account differences in PK between compounds. Through the $EC_{50}$ estimates—in principle the appropriate *in vivo* potency measure—the L6-OH appears five times more potent *in vivo* compared to lerisetron.

However, considering the unbound $EC_{50}$ ($EC_{50}u$) for both compounds, the relative potencies were equal. This agrees with *in vitro* results (10), where similar affinities of the two compounds for the $5\text{-}HT_3$ receptor ($pK_i$ = 9.2 and 9.0 for L and L6-OH, respectively) were obtained.

Besides the elevated potency of the metabolite, the generated concentrations, reached in blood after the effective dose of 10 μg $kg^{-1}$, are estimated to be low. However, it is still necessary to resolve the integrated PK/PD properties, so the kinetics of lerisetron and L6-OH was determined in conjunction. Then, the simulated PK (Fig. 9) is compared with the PD of Table III.

### Development of an Integrated L-L6-OH Model (PK-2)

Analyzing or modeling levels of systemically generated metabolite is difficult, so estimates of the L6-OH PK parameters were first obtained from its independent administration. An integrated PK model was fitted to the simultaneous concentration profiles of lerisetron and generated L6-OH following the administration of 200 μg $kg^{-1}$ lerisetron (i.v.). Although scarce, these models have shown to be of great use in establishing the contribution of active metabolites in the PK and the effect (midazolam, buspirone, morphine) (19,26–28).

The model permits the decomposition of lerisetron clearance into one part corresponding to the formation of L6-OH ($CL_{\rightarrow L6\text{-}OH}$ = 0.01384 L $min^{-1}$) and another encompassing the elimination through renal and other routes that is very small. The sum of these clearances yields a total clearance of 0.0139 L $min^{-1}$ for lerisetron, practically of the same order as that of standard PK analysis. It is concluded that the principal route of lerisetron elimination is the metabolic and mainly via hydroxylation into L6-OH, and to a lesser extent via renal and biliary routes, or conversion into other metabolites such as L5-OH. In fact, the fraction of lerisetron converted into metabolite ($F_c$, Eq. 11) was calculated at 99.6%, apparently contrasting with the low concentrations of L6-OH observed in plasma post-lerisetron dose. The integrated model verified the initial hypothesis that a large part of the formed L6-OH metabolite (a "first pass" effect) does not reach the general circulation but rather undergoes bile-to-feces excretion. This has been suggested for other drugs such as tolbutamide (29). This would explain the low concentrations in plasma of the metabolite after lerisetron i.v., and would also explain that, after $^{14}C$ lerisetron administration, most of the observed excretion is in feces.

Finally, with the PK parameters of lerisetron and its L6-OH metabolite, obtained with the integrated model, the contribution of the metabolite to the global effect of lerisetron was explored after a dose of 10 μg $kg^{-1}$, the highest dose used for the pharmacological effect of both compounds. The maximum simulated concentration for the metabolite was 0.057 ng $mL^{-1}$, less than the $EC_{50}$ estimated for the metabolite of 0.098 ng $mL^{-1}$. Even considering the unbound fraction of L6-OH in the presence of L (63%), the maximum unbound concentration would still be below the $EC_{50}u$. As early concentration observations of generated L6-OH showed magnitudes lower than the *in vitro* potency ($pK_i$), a competitive interaction PD model was not employed in the final analysis.

Therefore, we conclude that the contribution of L6-OH in the global effect of lerisetron in the rat is small, and this is mainly because the metabolite, once formed, does not reach the central compartment. Interestingly, this lack of significant effect is, besides the apparently increased potency of L6-OH, reflected in the $ED_{50}$s and even beyond that expected from knowledge only of the similar $EC_{50}u$. Solely, resolution of the PK together with the unbound PD permits prediction of the correct effect pointing to the role of combined PK/PD studies in drug development and therapy.

In summary, for a metabolite to contribute significantly to the clinical effect, it should have the following characteristics: (1) it should possess intrinsic activity (which applies to the case of L6-OH); (2) it should be formed in sufficient amounts after therapeutic doses of the drug (which refers to the case of lerisetron and its hydroxy metabolite); (3) it should possess PK properties such that it can reach sufficiently high concentrations at the site of action (which does not hold true for L6-OH). Therefore, as L6-OH does not contribute to the duration of the global effect, other administration routes are being explored for long-lasting therapy.

## ACKNOWLEDGMENTS

Funding for this study was provided in part by the Ministry of Science and Technology of Spain (PROFIT 2000–2003) and the Department of Industry, Commerce and Tourism of the Basque Government (INTEK 2002), and also

by a UPV group grant (9/UPV 00026-327-14593/2002). One of the authors (F.O.) was funded by a Gangoiti Foundation fellowship.

## REFERENCES


1. P. J. Hesketh. Comparative review of 5-$HT_3$ receptor antagonists in the treatment of acute chemotherapy-induced nausea and vomiting. *Cancer Invest.* **18**:163–173 (2000).
2. S. Goodin and R. Cunningham. 5-$HT_3$-receptor antagonists for the treatment of nausea and vomiting: a reappraisal of their side-effect profile. *The Oncologist* **7**:424–436 (2002).
3. R. E. Gregory and D. S. Ettinger. 5-$HT_3$ receptor antagonists for the prevention of chemotherapy-induced nausea and vomiting: a comparison of their pharmacology and clinical efficacy. *Drugs* **55**:173–189 (1998).
4. Y. E. Yarker and D. G. McTavish. Granisetron: An update of its therapeutic use in nausea and vomiting induced by antineoplastic therapy. *Drugs* **48**:761–793 (1994).
5. V. Fischer, J. P. Baldeck, and F. L. S. Tse. Pharmacokinetics and metabolism of the 5-hydroxytryptamine antagonist tropisetron after single oral doses in humans. *Drug Metab. Dispos.* **20**:603–607 (1992).
6. M. K. Reith, G. D. Sproles, and L. K. Cheng. Human metabolism of dolasetron mesylate, a 5-$HT_3$ receptor antagonist. *Drug Metab. Dispos.* **23**:806–812 (1995).
7. N. D. Evans, K. R. Godfrey, M. J. Chapman, M. J. Chappell, L. Aarons, and S. B. Duffull. An identifiability analysis of a parent–metabolite pharmacokinetic model for ivabradine. *J. Pharmacokinet. Pharmacodyn.* **28**:93–105 (2001).
8. M. Rowland and T. N. Tozer. *Clinical Pharmacokinetics: Concepts and Applications*, 3rd ed, Williams & Wilkins, Media, Pennsylvania, 1995, pp. 367-393
9. M. Cooper, A. Sologuren, R. Valiente, and J. Smith. Effects of lerisetron, a new 5-$HT_3$ receptor antagonist, on ipecacuanha-induced emesis in healthy volunteers. *Arzneim-Forsch./Drug Res.* **52**:689–694 (2002).
10. A. Orjales, R. Mosquera, L. Labeaga, and R. Rodes. New 2-piperazinylbenzimidazole derivatives as 5-$HT_3$ antagonists. Synthesis and pharmacological evaluations. *J. Med. Chem.* **40**:586–593 (1997).
11. J. R. Fozard and M. Host. Selective inhibition of the Bezold–Jarisch effect of 5-HT in the rat by antagonists at neuronal 5-HT receptors. *Br. J. Pharmacol.* **77**:520p, (1982).
12. M. Yamano, T. Kamato, A. Nishida, H. Ito, H. Yuki, R. Tsutsumi, K. Honda, and K. Miyata. Serotonin (5-HT) receptor antagonism of 4, 5, 6, 7-tetrahydrobenzimidazole derivatives against 5-HT induced bradycardia in anesthetized rats. *Jpn. J. Pharmacol.* **65**:241–248 (1994).
13. N. Jauregizar, R. Calvo, E. Suárez, A. Quintana, E. Raczka, and J. C. Lukas. Altered disposition and effect of lerisetron in rats with elevated alpha1-acid glycoprotein levels. *Pharm. Res.* **18**:838–845 (2001).
14. N. Jauregizar, R. Calvo, E. Suarez, A. Quintana, E. Raczka, and J. C. Lukas. Pharmacokinetics and pharmacological effect of lerisetron, a new 5-$HT_3$ antagonist, in rats. *J. Pharm. Sci.* **91**:41–52 (2002).
15. N. Jauregizar, A. Quintana, E. Suarez, E. Raczka, L. de la Fuente, and R. Calvo. Age-related changes in pharmacokinetics and pharmacodynamics of lerisetron in the rat: a population pharmacokinetic model. *Gerontology* **49**:205–214 (2003).
16. V. P. Shah, K. K. Midha, J. W. A. Findlay, H. M. Hill, J. D. Hulse, I. J. McGilveray, G. Mckay, K. J. Miller, R. N. Patnaik, M. L. Powell, A. Tonelli, C. T. Viswanathan, and A. Yacobi. Bioanalytical Methods validation—a revisit with a decade of progress. *Pharm. Res.* **17**:1551–1557 (2000).
17. R. Calvo, R. M. Jimenez, I. F. Troconiz, E. Suarez, A. Gonzalo, M. L. Lucero, E. Raczka, and A. Orjales. Serum protein binding of lerisetron, a novel specific 5-$HT_3$ antagonist, in patients with cancer. *Cancer Chemother. Pharmacol.* **42**:418–422 (1998).
18. L. B. Sheiner and S. L. Beal. Some suggestions for measuring predictive performance. *J. Pharmacokinet. Biopharm.* **9**:503–512 (1981).
19. K. P. Zuideveld, J. Rusiç-Pavletiç, H. J. Maas, L. A. Peletier, P. H. Van Der Graaf, and M. Danhof. Pharmacokinetic–pharmacodynamic modeling of buspirone and its metabolite 1-(2-pyrimidinyl)-piperazine in rats. *J. Pharmacol. Exp. Ther.* **303**:1130–1137 (2002).
20. D. K. Walker. The use of pharmacokinetic and pharmacodynamic data in the assessment of drug safety in early drug development. *Br. J. Clin. Pharmacol.* **58**:601–608 (2004).
21. D. A. Saynor and C. M. Dixon. The metabolism of ondansetron. *Eur. J. Clin. Oncol.* **25**(Suppl. 1):S75–S77 (1989).
22. C. M. Dixon, P. V. Colthup, C. J. Serabjit-Singh, B. M. Kerr, C. C. Boehlert, G. R. Park, and M. H. Tarbit. Multiple forms of cytochrome P450 are involved in the metabolism of ondansetron in humans. *Drug Metab. Dispos.* **23**:1225–1230 (1995).
23. M. T. Serafini, S. Puig, G. Garcia-Encina, R. Farran, A. Garcia-Soret, T. Moragon, and L. Martínez. Absorption, distribution and excretion of [14C]-lesopitron after single and repeated administration in rats and dogs. *Methods Find. Exp. Clin. Pharmacol.* **19**:61–72 (1997).
24. J. H. Lin and M. Yamazaki. Role of P-glycoprotein in pharmacokinetics. Clinical implications. *Clin. Pharmacokinet.* **42**:59–98 (2003).
25. C. Yamamoto, H. Murakami, N. Koyabu, H. Takanaga, H. Matsuo, T. Uchiumi, M. Kuwano, M. Naito, T. Tsuruo, H. Ohtani, and Y. Sawada. Contribution of P-glycoprotein to efflux of ramosetron a 5-$HT_3$ receptor antagonist, across the blood–brain barrier. *J. Pharm. Pharmacol.* **54**: 1055–1063 (2002).
26. B. Tuk, M. F. Van Oostenbruggen, V. M. M. Herben, J. W. Mandema, and M. Danhof. Characterization of the pharmacodynamic interaction between parent drug and active metabolite *in vivo*: Midazolam and α-OH-midazolam. *J. Pharmacol. Exp. Ther.* **289**:1067–1074 (1999).
27. J. Lötsch, C. Skarke, H. Schmidt, J. Liefhold, and G. Geisslinger. Pharmacokinetic modeling to predict morphine and morphine-6-glucuronide plasma concentrations in healthy young volunteers. *Clin. Pharmacol. Ther.* **72**:151–162 (2002).
28. B. P. Murthy, G. M. Pollack, and K. L. R. Brouwer. Contribution of morphine-6-glucuronide to antinociception following intravenous administration of morphine to healthy volunteers. *J. Clin. Pharmacol.* **42**:569–576 (2002).
29. S. B. Martin and M. Rowland. Determination of tolbutamide and metabolites in biological fluids. *Anal. Lett.* **6**:865–876 (1973).